Petrographic relationships between mineral phases and bitumen in the Oklo Proterozoic natural fission reactors, Gabon

JOHN PARNELL

School of Geosciences, Queen's University of Belfast, Belfast BT7 1NN, UK

Abstract

Several of the Proterozoic natural fission reactors at Oklo, Gabon contain abundant organic matter (bitumen), with which much of the reactor uranium is associated. An understanding of the petrography of the bitumen is important in assessing its role in element retention following fissiogenic reactions. The bitumen is replacive and includes vestiges of detrital grains and clays of the host sandstones. It also contains several generations of mineral phases related to the migration of uranium and daughter lead, and other elements mobilized by hydrothermal activity in the reactor zones. The minerals include (primary) uraninite precipitated after reduction of uranium by organic matter, silicates concentrated in radiation halos around the uraninite, and native lead, galena and further uraninite which migrated from the primary uraninite. The silicates are illitic clays in the immediate vicinity of the reactors, and chloritic more distant from the reactors. Authigenic clays in radiation halos are compositionally distinct from earlier host rock clays. Local migration of uranium and lead is evident as dispersion of the elements through the radiation halos; cross-cutting veinlets of uraninite, native lead and galena, including veinlets extending directly from the primary uraninite crystals; and concentrations of the elements at the margins of bitumen masses. The limit of observed uranium dispersion is within clay immediately beyond the bitumen margins.

KEYWORDS: natural fission reactors, bitumen, uranium, Oklo, Gabon.

Introduction

THE uranium ore deposits at Oklo, Gabon, are unique in including nearly twenty natural fission reactors, composed of high grade uranium ore and identified by a marked depletion in the isotope ^{235}U. They occur within the lower Proterozoic Francevillian Series, which reaches a maximum thickness of 4 km. The reactors are of great interest because they are the only known examples of nuclear fission products which have resided in a natural environment for a geologically long time: the short-lived fission products have decayed to more stable daughter products. Many of the reactors contain veinlets and irregular masses of migrated bitumen. Uranium mineralization may have been focussed by reservoir structures following oil generation and migration within the Francevillian rocks (Gauthier-Lafaye and Weber, 1981, 1989, 1993). Up to 60% uranium occurs in the richest ore bodies (Gauthier-Lafaye *et al.*, 1989), which became sites of nuclear fission reactors at about 2 Ga. Reaction zones are typically 10 m × 10 m and up to 50 cm thick. Water acted as a neutron moderator in the reactors, which ceased functioning when the water was expelled (Naudet, 1978). The resultant hydrothermal fluids caused alteration and fracturing at the reactor margins, which are consequently rich in clay minerals, and may have been responsible for further generation of hydrocarbons from kerogen in the country rock. There is certainly evidence for several generations of bitumen migration within the deposits (Nagy *et al.*, 1993). The bitumen occurs as interstitial pore-fillings, replacive nuggets and fracture-fillings in sandstones and conglomerates, commonly associated with calcite.

Much research has focussed upon the migration and retention of elements about the Oklo reactors. Work on fissiogenic isotopes shows that many fission products are retained at the site of production, and

Mineralogical Magazine, August 1996, Vol. 60, pp. 581–593

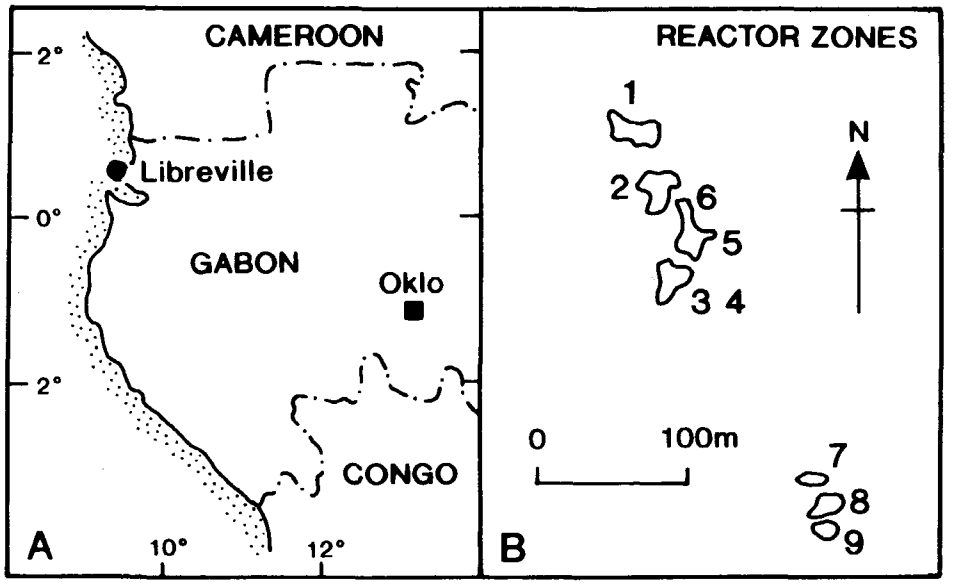

FIG. 1. A, Location of Oklo, Gabon, west Africa. B, Location of reactor zones 1 to 9 at Oklo (after De Laeter, 1985).

others have migrated but are retained at the reactor boundaries (Brookins, 1983, 1984; Curtis *et al.*, 1989; De Laeter *et al.*, 1980; Hemond *et al.*, 1992; Loss *et al.*, 1984). Uraninite in particular is known to retain many elements in the reactors (Ruffenach *et al.*, 1980). In the peripheral rocks, elements are probably fixed by a variety of authigenic minerals including clays, carbonates and sulphates (Brookins, 1983, 1984, 1990; De Laeter, 1985; Loss *et al.*, 1989). The clays in the reactors are considered to be analogues for artificial barrier clays around nuclear waste repositories (Brookins, 1990). However it has been suggested that some of the clay gangue may have been precipitated subsequent to the nuclear reactions, possibly through remobilization of ions during hydrothermal alteration (Loubet and Allegre, 1977; Maurette, 1976). Menet *et al.* (1992) calculated from bulk chemistries that clays in the reactor core and border massively retained many radioelements, and that other secondary minerals (including zircon, titanates, galena) may also act as traps for migrating elements. They also emphasized that the interface between the reactor border and the unaltered sandstone may be an efficient barrier to some elements because it marks a redox front between the oxidizing core and the surrounding reducing environment. The presence of organic matter is also significant to element migration, as retention is greater within organic-rich matrices (Hidaka *et al.*, 1993; Nagy *et al.*, 1991*b*, 1993).

The petrography of the bitumen has been studied by several workers, most of whom figured the numerous uraninite inclusions distributed through the bitumen (Alpern, 1978; Cassou *et al.*, 1975; Cortial *et al.*, 1990; Eberly *et al.*, 1994; Gauthier-Lafaye and Weber 1993; Geffroy, 1975; Mossman *et al.*, 1993; Nagy *et al.*, 1991b). Despite the substantial data available on bitumen petrography and element retention within the deposits, there is a relative lack of information on the petrographic relationships between bitumen and inorganic minerals. This account describes the relationships in samples from several reactors at Oklo, covering (i) the identification of mineral phases in bitumen, (ii) their paragenesis with each other and with the host bitumen, (iii) relationships with uranium/lead distribution, and (iv) inferences about the origin of the mineral phases.

Samples/methodology

Samples were examined from the vicinity of the cores of reactors 7, 8 and 9 (Fig. 1). They represent varying distances from the reactor cores. Their identity is summarized in Table 1. Samples were from batches distributed by Prof. Bartholemew Nagy (University of Arizona) to collaborating research groups. The bitumen examined is the abundant form described as OUA (organics of uncertain affinity) by Mossman *et al.* (1993).

TABLE 1. Identification of samples of organic matter (OM) studied from Oklo

GL 2728	OM in clay in reactor 7
GL 2753	pure OM beneath/against core of reactor 7
GL 2488	OM in sandstone 5cm from core of reactor 7
GL 2489	OM in sandstone 30 cm from core of reactor 7
TiV 292-1	pure OM 5 m from reactor 7
GL 3090	pure OM several m from reactor 8
KP 3	OM in clay/sandstone in core of reactor 9
GL 3001	OM in sandstone in core of reactor 9
GL 3165	OM from margin of reactor 9
GL 3141	OM in siltstone 1.5 m from reactor 9
ES 24/3	OM in sandstone 500 m from reactors 7–9

Samples of bitumen were mounted in resin on metal stubs and progressively polished down to 1 micron grade with diamond paste. The samples were then coated with carbon or gold and examined using a JEOL-733 electron microprobe and/or a JEOL-6400 scanning electron microscope, both in backscattered mode. Analytical work was undertaken using a beam diameter of 1 micron, with an accelerating voltage of 15 keV and a beam current of 15–25 nA.

Bitumen petrography

The bitumen examined occurs in massive and globular (Fig. 2*a*) form on a millimetre-scale within sandstones and microconglomerates. At the margins

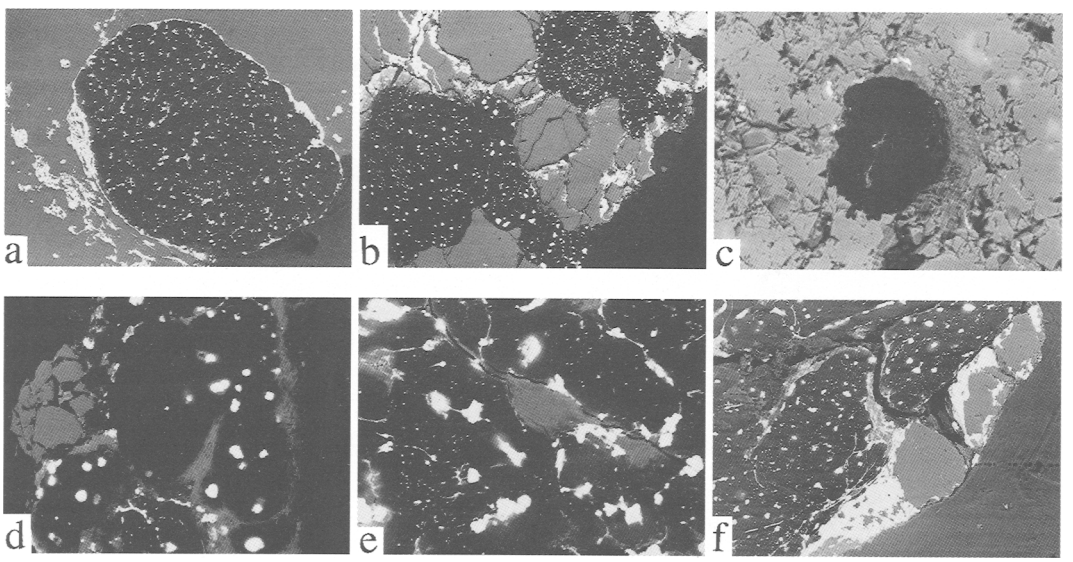

FIG. 2. Electron micrographs showing relationships between bitumen (black) and host rock. A, Bitumen nodule containing abundant uraninite inclusions, with concentration of uraninite (bright) at boundary with host chlorite. (sample GL 2728, field width 1.3 mm). B, Coalesced nodules of bitumen containing uraninite inclusions; fractures in host quartz filled with uraninite/galena. (sample ES 24/3, field width 2.8 mm). C, Bitumen nodule with very few inclusions, exhibiting penetrative replacement into quartz host. (sample GL 2489, field width 240 μm). D, Coalesced nodules of bitumen in illitic clay/quartz host; smaller nodules developed around single crystals of uraninite; quartz (left margin) broken and penetrated by bitumen. (sample GL 2488, field width 380 μm). E, Mass of residual illitic clay trapped within bitumen mass. (sample GL 3165, field width 260 μm). F, Massive galena (G) precipitated at boundary of bitumen mass with quartz host. (sample GL 3001, field width 1.0 mm).

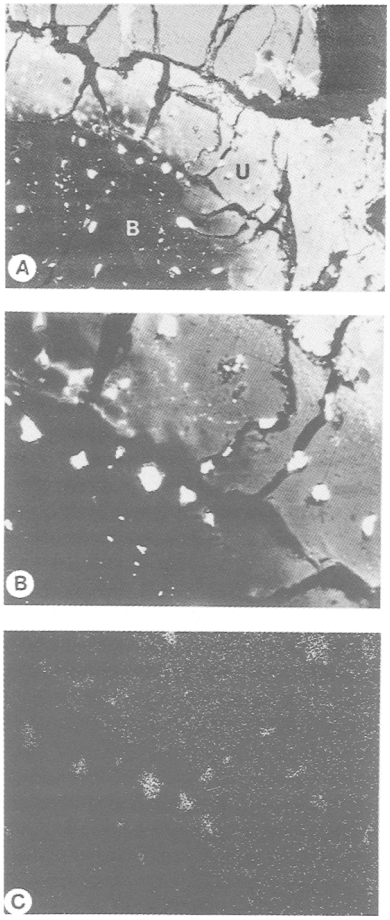

FIG. 3. Margin of bitumen mass, showing transition from normal bitumen (black, B) to oxidized zone (pale, U) at margin with host quartz. A, field width 1.0 mm. B, close-up field width 370 mm. C, uranium X-ray map of field in B, showing clear uranium enrichment in oxidized zone. (sample GL 3001).

of massive bitumen, the massive form appears to be a product of coalescence of globular bitumen (Fig. 2*b*). The bitumen is a brittle solid of negligible solubility in organic solvents, and reflectance above 2% (detailed reflectance data in Mossman *et al.*, 1993). The reflectance increases around some uraninite inclusions. In samples from both near reactor 7 (TiV 292-1) and distant from the reactor (ES 24/3), some portions of bitumen exhibit bright back-scattered images rather than the black images typical of organic materials (Fig. 2*c*) due to extensive oxidation and accompanying enrichment in uranium (Fig. 3).

Bitumen globules show a replacive relationship with the detrital grains, which are almost exclusively rounded quartz grains replaced to varying degrees by clay minerals. Bitumen/quartz boundaries appear very irregular (Fig. 2c) due to penetrative replacement of quartz by the bitumen. The replacive habit of the bitumen results in vestiges of quartz/clay trapped near the margins of bitumen masses, or between coalesced bitumen masses.

Mineral phases

The sandstones which host the uranium ores and bitumen contain quartz grains, biotite, an illite/chlorite matrix, and variable cements of quartz overgrowth, hematite, dolomite and sulphates. The ore in the reactor cores has a gangue of clay minerals, whereas the normal uranium ore occurs within sandstone. The clays were produced by hydrothermal alteration of the sandstones, effected by the heat of nuclear fission reactions (Gauthier-Lafaye *et al.*, 1989). Quartz was dissolved at the reactor cores, and at the reactor margins vestiges of incompletely dissolved quartz are mixed with clay, uraninite, organic matter and resistate phases (zircon, etc.).

Inorganic phases found in direct relationship with the bitumen include quartz, uraninite, secondary uranium minerals, galena, native lead, clays, zircon and other heavy minerals. Quartz is generally the host detrital mineral but is rarely present within the bitumen masses. The predominant mineral within the bitumen masses is uraninite. The size of uraninite crystals varies up to 70 μm, and crystals are generally of comparable size within a portion of bitumen (Fig. 2*a*). Equigranular and equidimensional uraninite crystals are distributed evenly through the bitumen, i.e. in an equidistant manner. Between the uraninite crystals are abundant micron-scale galena crystals, also disseminated evenly through the bitumen. The smallest bitumen globules are developed around single uraninite crystals (Fig. 2*d*). Bitumen globules beyond the reactor margins may contain a relatively sparse distribution of uraninite crystals (Fig. 2*c*). Rarely, a uranium-titanium phase (composition akin to brannerite) occurs within the bitumen, but this is much more abundant outside the bitumen in the host rock.

The larger uraninite crystals in particular exhibit halos within the host bitumen, characterized by a lighter image in backscattered mode (Fig. 4), and regarded as radiation halos (see below). Some halos are complete and of constant thickness; others are developed irregularly around only parts of the uraninite crystal. The radiation halos confer an anisotropy to the bitumen, which is reflected in the distribution of other mineral phases. Mineral annuli occur around the equidimensional uraninite crystals, usually beyond the observed limit of the radiation

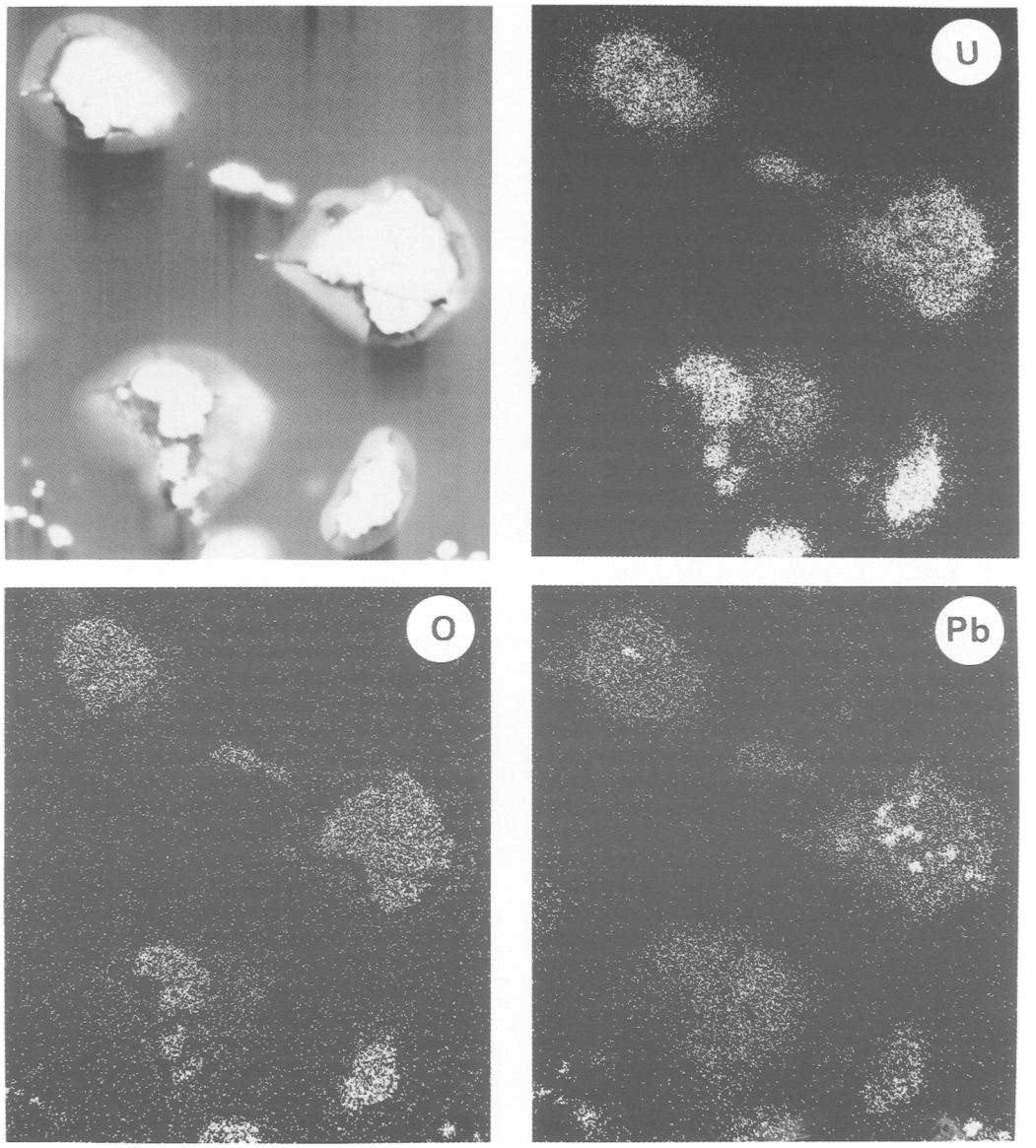

FIG. 4. Electron image and U/O/Pb X-ray maps of uraninite crystals and their radiation halos. Halos are enriched in uranium and lead. (sample GL 3090, field width 120 μm).

halos (Figs 5*a*, 6). The annuli consist of further uraninite plus galena, native lead and some clay. Galena and native lead also occur in annular structures at a distance of up to 50 μm from the uraninite core. The lead phases also occur as discrete phases within or at the margin of the larger uraninite crystals, and as randomly distributed crystals within the bitumen.

Clay minerals occur in several settings; as large masses which enclose some bitumen masses and appear to be trapped between coalesced bitumen masses (Fig. 7) (in three dimensions they may be exterior to the bitumen), as small masses completely isolated within the bitumen (Figs 2*e*, 5*b*), and as growths on the surface of larger uraninite crystals. The clays on the surface of uraninite crystals occur

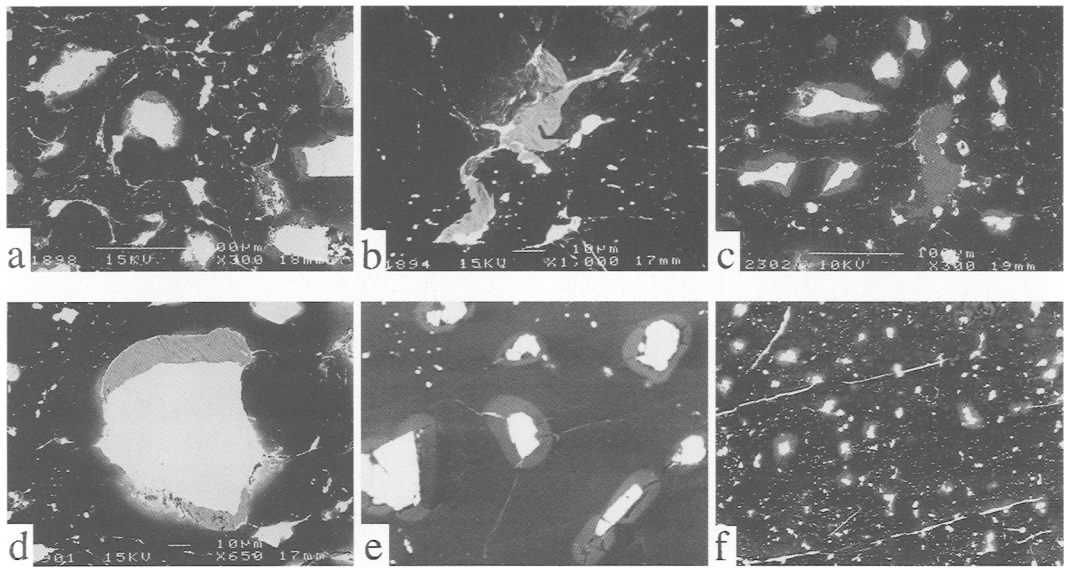

FIG. 5. Electron micrographs showing mineral inclusions within bitumen (black). A, Anisotropy developed around large uraninite crystal, which caused mineral precipitation (further uraninite, native lead, galena, clay) in annular pattern; smaller crystals also exhibit circum-uraninite mineral distribution. (sample GL 3165, field width 380 μm). B, Irregular mass of authigenic illite within bitumen. Isolated illite crystals beyond margin of mass (arrowed). (sample GL 3165, field width 115 μm). C, Numerous large uraninite crystals with partial coatings of illitic clay, and separate irregular mass of authigenic clay. (sample GL 3165, field width 380 μm). D, Large uraninite crystal with partial coating of illitic clay; outer margin of clay shows very thin coating of uraninite/galena. (sample GL 3165, field width 175 μm). E, Uraninite crystal (centre) with radiating veinlets of galena. (sample GL 3090, field width 210 μm). F, Bitumen containing abundant inclusions of uraninite and galena, with cross-cutting parallel veinlets of galena. (sample GL 3001, field width 570 μm).

within the radiation halos (Fig. 5*c,d*) and also beyond them, but they are only present in samples from the immediate vicinity of the reactors. The clay mineralogy is a mixture of potassium-rich and iron/magnesium-rich phases, identified as illite and chlorite respectively (Table 2). Most samples from the cores of reactors 7 and 9 contain illite, while other samples contain illite or mixtures of illite and chlorite. In a detailed study of the clay phases in sample GL 3165 from the margin of reactor 9, there is a clear distinction between the composition of the residual (trapped) clays and the clays on the uraninite surfaces. The halo clays are relatively rich in potassium compared to the residual clays (Fig. 8, Table 2). There were no detectable levels of cations heavier than iron. Both illite and chlorite are found among the residual clays, but the halo clays and other authigenic clay growths are consistently illite. The illite contains up to 4 atomic % potassium, equivalent to 8 wt.% K_2O (Table 2). In the clearest examples of halo clays, clay crystals appear to be orientated normal/sub-normal (never tangential) to the uraninite surfaces as

TABLE 2. Typical analyses (weight %) of authigenic clay phases in bitumen at Oklo

	1	2	3	4	5
K_2O	0.20	4.65	5.31	7.88	0.03
CaO	0.28	0.03	0.00	0.00	0.13
Fe_2O_3	9.20	1.24	1.43	1.02	18.13
MgO	1.83	1.21	0.60	0.96	9.20
Na_2O	0.00	0.25	0.20	0.36	0.00
TiO_2	0.06	0.45	0.53	0.16	0.35
Al_2O_3	37.73	37.31	31.28	33.57	32.74
SiO_2	42.91	48.93	45.78	46.33	37.48
Total	92.20	94.07	85.13	90.27	98.07

1. GL 3165 residual clay (chlorite)
2. GL 3165 halo clay (illite)
3. ES 24/3 authigenic illite
4. GL 2489 authigenic illite
5. GL 2728 host chlorite.

Oxide percentages calculated assuming stoichiometry.

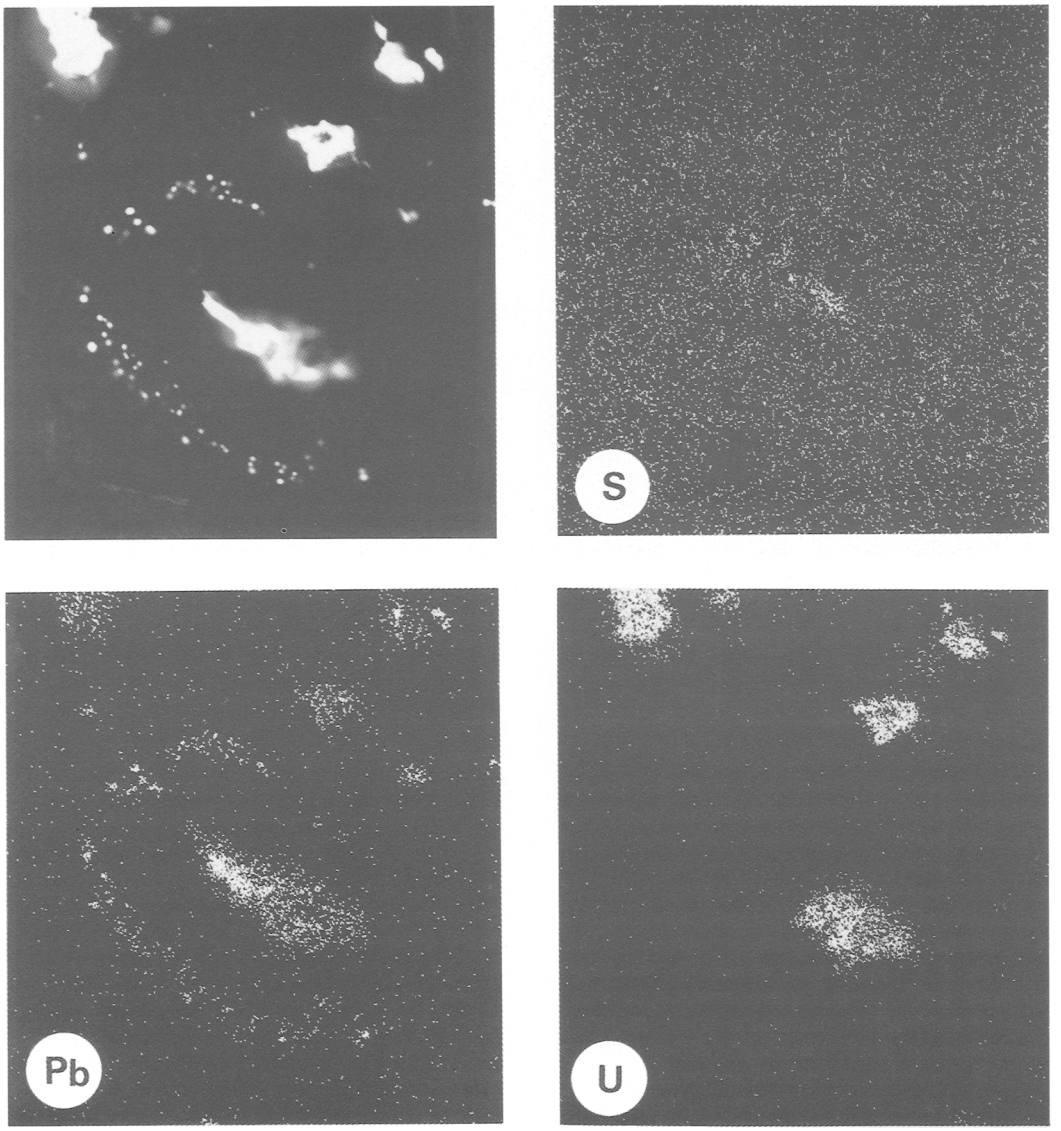

FIG. 6. Electron image and S/Pb/U X-ray maps showing annular distribution of lead inclusions around uraninite crystal. Sulphur distribution indicates native lead rather than galena. Lead distribution also indicates enrichment in uraninite crystals. (sample KP 3, field width 130 μm).

if nucleated on those surfaces (Fig. 5*d*). The small isolated masses of clay (commonly 1–3 microns crystal size) are individual lath-shaped crystals or coalesced crystals which appear to be authigenic precipitates. Some isolated masses of clay form part of the annuli of minerals around large uraninite crystals (Fig. 5*a*). Some clay analyses yield up to 1 atomic % vanadium, particularly in the illitic clays.

The observation of radiation halos in electron images indicates that the halos differ chemically from the adjacent bitumen. X-ray maps indicate some dispersion of uranium into the halos, a stronger dispersion of lead, and in some cases an increased content of oxygen (*N.B.* some apparent element enrichment in the halo arises where X-rays penetrate a uraninite crystal which is larger below the sample

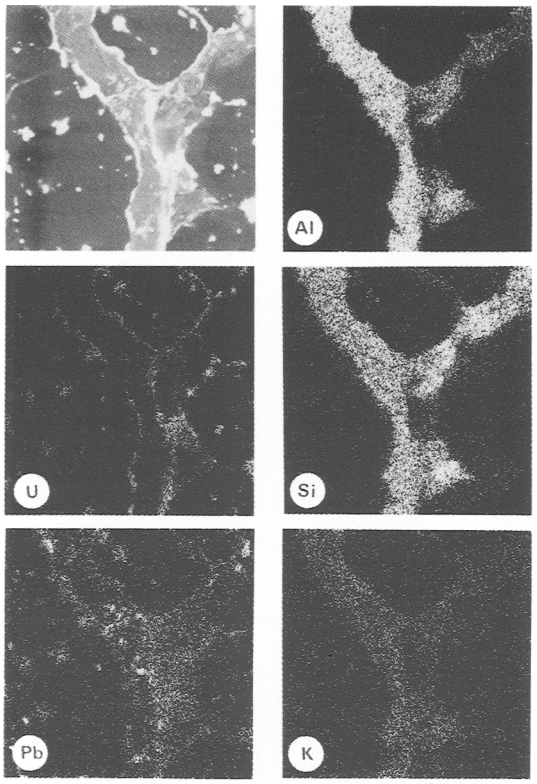

FIG. 7. Electron image and Al/U/Si/Pb/K X-ray maps of host clay between bitumen masses. Maps show that clay varies in composition, uranium and lead are concentrated at bitumen/clay boundary, and lead is dispersed into clay. (sample GL 3001, field width 250 μm).

surface). Where clay coats the uraninite, there may be an enrichment in uranium, lead and oxygen in the halo beyond the clay (Fig. 9). The intervening clay does not exhibit these enrichments.

Where clay coatings on uraninite extend beyond the radiation halo, the outer margin of clay may be rimmed by uraninite/galena/native lead. At the edge of the whole bitumen masses, concentrations of uranium and lead occur at the interface between bitumen and quartz/clay (Figs 2*f*, 7). Native lead/galena are commonly predominant at the interface, and lead shows greater dispersion into the adjacent mineral than uranium.

Veinlets of native lead, galena and uraninite also occur within the bitumen and extending into the host rock. The cross-cutting veinlets can be grouped into two categories. Some have arcuate to irregular shapes and in some cases can be seen extending directly from the primary uraninite crystals (Fig. 5*e*). These veinlets extend to distances up to several times the observable width of the radiation halos. Many halos contain empty cracks, radiating away from the uraninite crystals: these cracks may have been empty since formation, although loss of mineral infilling during sample preparation is also possible. The second type of veinlet is planar and occurs in groups which are parallel to each other and extend from the bitumen into the host rock. The veinlets are particularly common in bitumen which is rich in disseminated micron-scale galena crystals (Fig. 5*f*).

Discussion

Mineral phases. The large uraninite crystals are directly related to the bitumen masses, particularly where single crystals occur at the core of small masses. This suggests a genetic relationship, specifically precipitation of the uraninite from within the bitumen (see below).

The later mineral phases are related particularly to the distribution of uraninite crystals and their surrounding radiation halos. Radiation halos are widely observed in organic materials around uranium-bearing minerals using optical microscopy, and they are generally attributed to increases in hardness and reflectance due to radiation damage (Leventhal *et al.*, 1986, 1987). The halos evident in electron images reflect chemical variations rather than physical alteration, but the halos figured here are of comparable dimensions to those observed in reflected light. The concentrations of oxygen in the radiation halos indicate oxidation of the organic matter which was probably a consequence of radiolysis (decomposition of material by irradiation, notably of water into oxygen and hydrogen). The general chemistry and mineralogy of the reactor cores indicates that conditions were oxidising, in contrast to the surrounding environment (see above).

The uraninite/native lead/galena at the outer rim of the uraninite-coating clays indicates migration of uranium and lead through the clay. This may have been facilitated by the metamict nature of the clay (see below). It is expected that the clay in close contact with the uraninite would be metamict (Durrance, 1986). Some clays at Oklo have been determined to be fully crystalline and not metamict (Maurette, 1976), but such measurements need to be made upon individual clay phases rather than bulk clay extractions. Clays in high-grade uranium ores elsewhere are metamict (Rimsaite, 1978, 1982). X-ray maps indicate that some uranium is located within the Oklo clays. Clay minerals are capable of uranium levels up to several per cent (Rimsaite, 1982). While the metamict state might give rise to abundant sites which could accommodate metals, such sites would not be very stable and metal migration through the clay could be relatively easy.

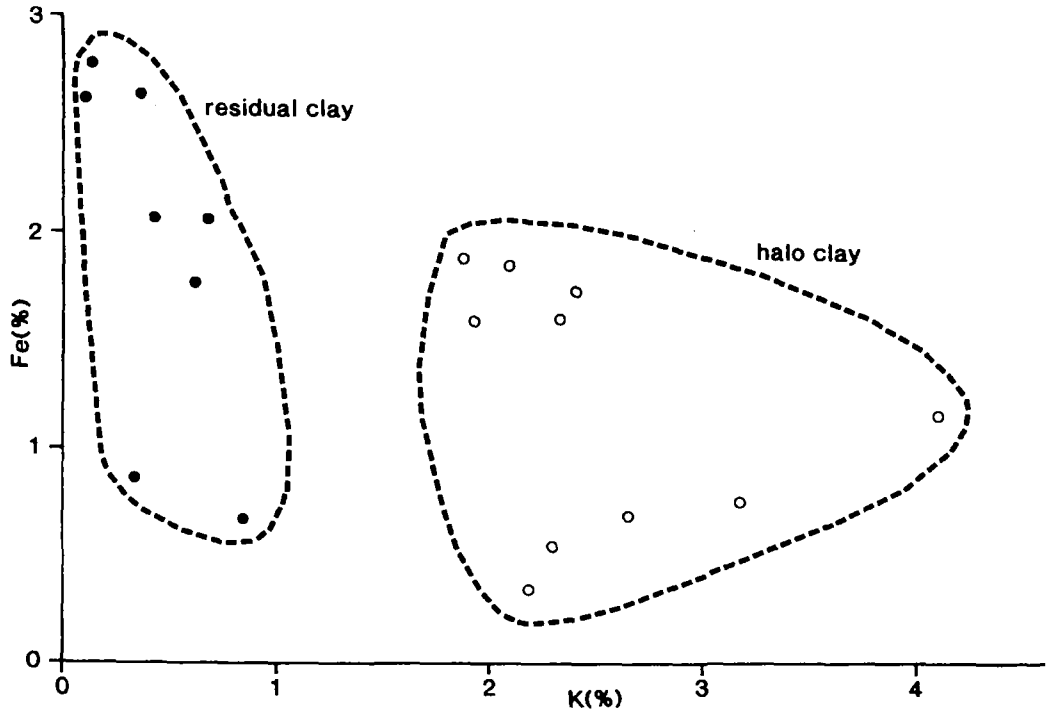

FIG. 8. Cross-plot of potassium and iron atomic percentages in two types of clay in sample GL 3165, showing their distinct composition.

Circum-uraninite cracks, and mineral precipitation therein, are typically 20–50 μm beyond the edge of uraninite crystals. This is comparable with 50-μm width radiation halos in Canadian bitumen measured by Leventhal *et al.* (1987) and the 40–60 μm range for alpha particle penetration into organic matter (Friedlander and Kennedy, 1962). These observations suggest that the cracks are related to alteration of the organic matter by irradiation. Other work in this laboratory shows that the control on mineral distribution by anisotropy through radiation damage around uraninite crystals is not unique. In the uranium-rich kolm nodules in the Alum Shales of Sweden (Parnell, 1984), the minerals are distributed in a markedly concentric manner about brannerite crystals (Fig. 10).

Previous observations of clay mineralogy report that illite is developed at the focus of intense alteration in the reactor core and that chlorite is the predominant clay phase beyond the core (Gauthier-Lafaye *et al.*, 1989; Menet *et al.*, 1992). However, the detailed observations made in this study indicate that the authigenic clays are consistently illitic. Identifications of the host clay mineralogy also do not fit the simple trend previously recorded. For example, sample GL 2728 from reactor 7 is chloritic, while illite is the predominant clay in sample ES 24/3 500m distant from the reactor.

The trace quantities of vanadium in authigenic clays are typical of clays from uranium deposits in continental 'red bed' sandstones. Potassic clays can accommodate several per cent vanadium in the mineral roscoelite (Fischer *et al.*, 1947). Discrete vanadium minerals are also recorded in the Oklo deposits (Gauthier-Lafaye and Weber, 1989), reflecting the control of uranium and vanadium behaviour by similar redox conditions, i.e. mobility in oxidizing environments and deposition in reducing environments.

The two types of veinlet of uraninite/native lead/galena cutting across the bitumen have different origins. The irregular veinlets extending from uraninite crystals are infillings of cracks generated within the radiation halos and then perpetuated beyond into the surrounding bitumen. Similar cracks have been observed around uranium minerals elsewhere (Rimsaite, 1982), and are probably a shrinkage feature accompanying maturation of the

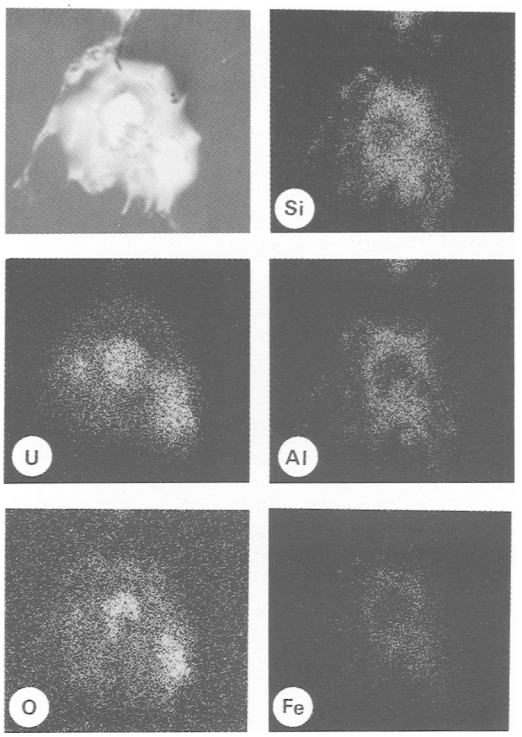

FIG. 9. Electron image and Si/U/Al/O/Fe X-ray maps of clay and radiation halo around uraninite crystal. Si/Al/Fe identifies clay phase; radiation halo enriched in uranium and oxygen. (sample GL 2488, field width 75 μm).

bitumen by irradiation. The parallel planar veinlets are infillings of a brittle fracture system which affects both bitumen and host rock.

There is no clear pattern to the relative distribution of galena and native lead. Sulphur is available in organic form within the bitumen, so that daughter lead from the decay of uranium can readily precipitate as galena.

Uranium-titanium phases are generally secondary (e.g. Smits, 1992); their greater abundance outside the bitumen may reflect the availability of titanium from titanium oxides in the sandstone host to the bitumen.

Mineral paragenesis and origin. The petrographic relationships suggest several generations of minerals within the bitumen: (i) vestiges of minerals, predominantly quartz and replacement clays and occasional heavy mineral grains, remaining after replacement of detrital grains by the bitumen; (ii) uraninite crystals precipitated soon after interaction between uraniferous fluids and the bitumen; (iii) precipitation of clays, particularly in anisotropic regions around uraninite crystals; (iv) disseminated galena, which was probably deposited over a long time period due to radioactive decay; (v) uraninite/native lead/galena at the margins of clay masses, and native lead/galena infills of brittle fractures cross-cutting the bitumen.

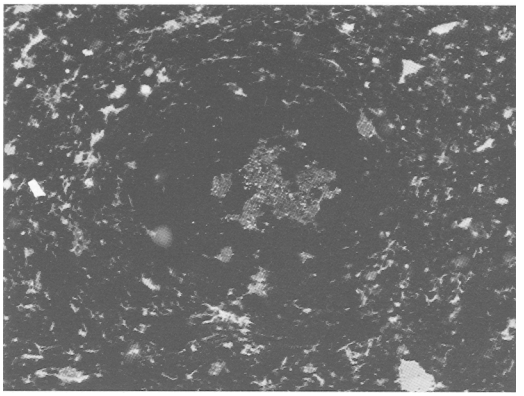

FIG. 10. Annular mineral distribution around brannerite crystal in kolm nodule, Swedish Alum Shales, analogous to distribution recorded in Oklo bitumen nodules. (field width 170 μm).

The observations of replacement of the host rock, and of individual minerals, are an almost ubiquitous feature of radioelement-bearing bitumens, whether uraniferous (Parnell and Eakin, 1987) or thoriferous (Parnell *et al.*, 1990). This consistent association indicates that some aspect of irradiation is responsible. A possible explanation is that large quantities of free radicals generated by radiolysis cause extensive corrosion of mineral surfaces. Breakdown of crystal lattices by irradiation to a metamict state would also make the minerals more susceptible to reaction.

As in many other uraniferous bitumens, the uraninite crystals are distributed evenly through the Oklo bitumen. This suggests precipitation of the uraninite from within the bitumen. Such a precipitation of uraninite from a highly uranium-rich bitumen has been induced experimentally (Rouzaud *et al.*, 1980). The enrichment of the bitumen would have been achieved by reduction of uranium from local groundwaters. The disseminated galena crystals represent the daughter products of radioactive decay.

Subsequent mineral precipitation depended upon the anisotropy around the uraninite crystals. It is difficult to assess the time needed for this anisotropy to develop, but Eakin (1989) indicated a lack of such features in rocks younger than Jurassic, i.e. a time of about 150 million years.

The ions comprising the authigenic silicate phases could be a residue of the large quantities mobilized

during hydrothermal alteration around the reactors. Alternatively some could be very locally derived following the replacement of host rock clays by the bitumen. The restriction of uraninite-coating clays to the immediate vicinity of the reactors suggests that the severe alteration around the cores was responsible for ion availability.

The last identifiable phases are the uraninite/native lead/galena precipitated following migration of metals to the margins of the clay growths and the margins of the whole bitumen masses, and the lead minerals in cross-cutting fractures. It is not possible to determine a time relationship between these, and they may have both precipitated over a long time period. The relationships of these later phases to the primary uraninite (including radiating veinlets, circum-uraninite distribution) strongly suggests that the later phases are migration products from the uraninite. There is no reason to invoke a new introduction of uranium from outside the bitumen.

Uranium and lead migration. The X-ray maps indicate that migration of uranium and daughter lead has occurred from the uraninite crystals. The uranium and lead in the radiation halos represent short range migration from the uraninite core (note ion microprobe scans presented by Nagy *et al.* (1993) did not detect this uranium migration). The uranium and lead in the circum-uraninite cracks indicates migration beyond the detectable radiation halos, although the cracks probably represent irradiation-induced anisotropy. The uranium and lead minerals at the boundaries of bitumen masses with host clay/quartz suggest precipitation at a redox interface. Although the metals at these boundaries could conceivably have migrated from outside, circumstantial evidence indicates that they were precipitated after migration through the bitumen to the margin. The dispersion of lead into clay beyond the boundary, to a greater degree than uranium, supports this conclusion. Enrichments in uranium/lead occur particularly at the margin of the bitumen (Fig. 2*f*), probably also following outward migration.

The uraninite and lead minerals in cross-cutting veinlets is also clear evidence for metal migration. The parallel veinlets which extend into the host rock could be related to dyke intrusion at about 1100 Ma, which is known to have been a period of uranium and/or lead mobility (Nagy *et al.*, 1991*a*). However, given the age of the Oklo deposits there have probably been other circumstances when fracturing was possible. The evidence for migration of uranium and lead, and accompanying fractionation, is consistent with the isotopic data which suggests a complex history for the uranium/lead system following initial mineralization (Lancelot *et al.*, 1975), although it is not possible to use petrographic data to confirm any particular history.

Conclusions

The bitumen masses contain a variety of mineral inclusions, which can be divided according to the following paragenetic sequence: (i) irregular patches of quartz and clay which survived replacement of the host sandstone/microconglomerate by bitumen; (ii) uraninite which precipitated after uptake into the bitumen of uranium which had been reduced from uranium-rich groundwaters; (iii) authigenic clays which precipitated especially within radiation halos around the uraninite crystals, and in circum-uraninite fractures. The clays are illitic, and are compositionally distinct from the residual clays trapped during replacement of the host rock; (iv) progressive radioactive decay of the uranium caused precipitation of daughter lead throughout the bitumen as disseminated galena; (v) further uraninite/native lead/galena precipitated at the outer margin of halo clays, at the boundaries of whole bitumen masses, and in fractures cross-cutting the bitumen.

Several of the petrographic observations are significant to the secondary distribution of lead and uranium: (i) galena is disseminated through the bitumen; (ii) radiation halos exhibit dispersion of uranium and lead from the core uraninite; (iii) uraninite and galena accumulated at the margins of halo clays, after migration through the clays; (iv) veinlets of uraninite/native lead/galena extend directly outwards from large uraninite crystals; (v) uraninite, native lead and galena precipitated at the boundaries of bitumen masses with the host quartz/clay, which may have represented a redox boundary; (vi) cross-cutting parallel veinlets of uraninite/native lead/galena represent infilling of brittle fractures.

These observations confirm isotopic evidence that mobilization of lead and uranium occurred, but document for the first time the various relationships of local lead and uranium migration with the detailed petrography of bitumen in the Oklo deposits.

Much research work on the Oklo reactors is related to their potential as analogues for nuclear waste containment (Brookins, 1990; Nagy *et al.*, 1991*a*; Nagy and Rigali, 1993). The petrographic data have emphasised the importance of organic matter in retaining fissiogenic products until the regional igneous/tectonic event, and is consistent with previous observations that the clays are less effective than organic matter in this retention (Nagy *et al.*, 1991*a*).

Acknowledgements

I am grateful to G. Alexander, P. Gaffikin and the staff of the Queen's University Electron Microscopy Unit for skilled techincal support. Oklo samples were provided by B. Nagy and J. Leventhal. The manu-

script benefitted from reviews by P. Wignall and an anonymous reviewer.

References

Alpern, B. (1978) Etude petrographique de la matière organique d'Oklo. In *Les Reacteurs de Fission Naturels*. IAEA-TC-119, Vienna, 333–51.

Brookins, D.G. (1983) Migration and retention of elements at the Oklo natural reactor. *Environment. Geol.*, **4**, 201–8.

Brookins, D.G. (1984) *Geochemical Aspects of Radioactive Waste Disposal*. Springer-Verlag, Berlin.

Brookins, D.G. (1990) Radionuclide behaviour at the Oklo nuclear reactor, Gabon. *Waste Management*, **10**, 285–96.

Cassou, A.-M., Connan, J., Correia, M. and Orgeval, J.-J. (1975) Etudes chimiques et observations microscopiques de la matière organique de quelques mineralisations uranifères. In *Le Phénomène d'Oklo*. IAEA- SM-204, Vienna, 195–206.

Cortial, F., Gauthier-Lafaye, F., Oberlin, A., Lacrampe-Couloume, G. and Weber, F. (1990) Characterization of organic matter associated with uranium deposits in the Francevillian Formation of Gabon (Lower Proterozoic). *Org. Geochem.*, **15**, 73–85.

Curtis, D., Benjamin, T., Gancarz, A., Loss, R., Rosman, K., De Laeter, J., Delmore, J.E. and Maeck, W.J. (1989) Fission product retention in the Oklo natural fission reactors. *Appl. Geochem.*, **4**, 49–62.

De Laeter, J.R. (1985) The Oklo reactors: natural analogues to nuclear waste repositories. *Search*, **16**, 193–6.

De Laeter, J.R., Rosman, K.J.R. and Smith, C.L. (1980) The Oklo natural reactor: cumulative fission yields and retentivity of the symmetric mass region fission products. *Earth Planet. Sci. Letters*, **50**, 238–46.

Durrance, E.M. (1986) *Radioactivity in Geology, Principles and Applications*. Wiley, London.

Eakin, P.A. (1989) Isotopic and petrographic studies of uraniferous hydrocarbons from around the Irish Sea Basin. *J. Geol. Soc., Lond.*, **146**, 663–73.

Eberly, P., Janeczek, J. and Ewing, R.C. (1994) Petrographic analysis of samples from the uranium deposit at Oklo, Republic of Gabon. *Radiochim. Acta*, **66**, 455–61.

Fischer, R.P., Hall, J.C. and Rominger, J.F. (1947) Vanadium deposits near Placerville, San Miguel County, Colorado. *Colorado Sci. Soc. Proc.*, **15**, 115–34.

Friedlander, G. and Kennedy, J.W. (1962) *Nuclear and Radiochemistry*. Wiley, New York.

Gauthier-Lafaye, F. and Weber, F. (1981) Les concentrations uranifères du Francevillien du Gabon: leur association avec des gites a hydrocarbures fossiles du Proterozoique inferieur. *Comptes Rendus Acad. Sci.*, **292**, 69–74.

Gauthier-Lafaye, F. and Weber, F. (1989) The Francevillian (Lower Proterozoic) uranium ore deposits of Gabon. *Econ. Geol.*, **84**, 2267–85.

Gauthier-Lafaye, F. and Weber, F. (1993) Uranium-hydrocarbon association in Francevillian uranium ore deposits, Lower Proterozoic of Gabon. In *Bitumens in Ore Deposits*, J. Parnell, H. Kucha and P. Landais, eds. Springer-Verlag, Berlin, 276–86.

Gauthier-Lafaye, F., Weber, F. and Ohmoto, H. (1989) Natural fission reactors of Oklo. *Econ. Geol.*, **84**, 2286–95.

Geffroy, J. (1975) Etude microscopique des minerais uranifères d'Oklo. In *Le Phénomène d'Oklo*. IAEA-SM-204, Vienna, 133–51.

Hemond, C., Menet, C. and Menager, M.T. (1992) U and Nd isotopes from the new Oklo reactor 10 (Gabon): evidence for radioelements migration. *Materials Research Society Symposium Proceedings*, **257**, 489–96.

Hidaka, H., Holliger, P. and Masuda, A. (1993) Evidence of fissiogenic Cs estimated from Ba isotopic deviations in an Oklo natural reactor zone. *Earth Planet. Sci. Letters*, **114**, 391–6.

Lancelot, J.R., Vitrac, A. and Allegre, C.J. (1975) The Oklo natural reactor: age and evolution studies by U-Pb and Rb-Sr systematics. *Earth Planet. Sci. Letters*, **25**, 189–96.

Leventhal, J.S., Daws, T.A. and Frye, J.S. (1986) Organic geochemical analysis of sedimentary organic matter associated with uranium. *Appl. Geochem.*, **1**, 241–7.

Leventhal, J.S., Grauch, R.I., Threlkeld, C.N., Lichte, F.E. and Harper, C.T. (1987) Unusual organic matter associated with uranium from the Claude deposit, Cluff Lake, Canada. *Econ. Geol.*, **82**, 1169–76.

Loss, R.D., Rosman, K.J.R. and De Laeter, J.R. (1984) Transport of symmetric mass region fission products at the Oklo natural reactors. *Earth Planet. Sci. Letters*, **68**, 240–8.

Loss, R.D., Rosman, K.J.R., De Laeter, J.R., Curtis, D.B., Benjamin, T.M., Gancarz, A.J., Maeck, W.J. and Delmore, J.E. (1989) Fission-product retentivity in peripheral rocks at the Oklo natural fission reactors, Gabon. *Chem. Geol.*, **76**, 71–84.

Loubet, M. and Allegre, C.J. (1977) Behaviour of the rare earth elements in the Oklo natural reactor. *Geochim. Cosmochim. Acta*, **41**, 1539–48.

Maurette, M. (1976) Fossil nuclear reactors. *Annual Review of Nuclear Science*, **26**, 319–50.

Menet, C., Menager, M.T. and Petit, J.C. (1992) Migration of radioelements around the new nuclear reactors at Oklo: analogies with a high-level waste repository. *Radiochimica Acta*, **59**, 395–400.

Mossman, D.J., Nagy, B., Rigali, M.J., Gauthier-Lafaye, F. and Holliger, P. (1993) Petrography and paragenesis of organic matter associated with the

natural fission reactors at Oklo, Republic of Gabon: a preliminary report. *Int. J. Coal Geol.*, **24**, 179–94.

Nagy, B., Gauthier-Lafaye, F., Holliger, P., Davis, D.W., Mossman, D.J., Leventhal, J.S., Rigali, M.J. and Parnell, J. (1991*a*) Organic matter and containment of uranium and fissiogenic isotopes at the Oklo natural reactors. *Nature*, **354**, 472–5.

Nagy, B., Leventhal, J.S. and Gauthier-Lafaye, F. (1991b) Organic geochemical and petrological investigations of a natural reactor and its environs at Oklo, Gabon: a preliminary report. *U. S. Geol. Surv. Circular*, **1058**, 65–7.

Nagy, B., Gauthier-Lafaye, F., Holliger, P., Mossman, D.J., Leventhal, J.S. and Rigali, M.J. (1993) Role of organic matter in the Proterozoic Oklo natural fission reactors, Gabon, Africa. *Geology*, **21**, 655–8.

Nagy, B. and Rigali, M.J. (1993) Newly discovered, organic matter-rich natural fission reactors at Oklo and Bangombé: Are they useful analogs for long-term anthropogenic nuclear waste containment? *WM '93 Conference Proceedings*, Tucson, 897–900.

Naudet, R. (1978) Conclusion sur le déroulement du phénomène. In *The Natural Fission Reactors*. Int. Atomic Energy Agency, Vienna, 715–34.

Parnell, J. (1984) The distribution of uranium in kolm: evidence from backscattered electron imagery. *Geol. Forenin. i Stockholm Forhandl.*, **106**, 231–4.

Parnell, J., and Eakin, P. (1987) The replacement of sandstones by uraniferous hydrocarbons: Significance for petroleum migration. *Mineral. Mag.*, **51**, 505–15.

Parnell, J., Monson, B. and Tosswill, R.J. (1990) Petrography of thoriferous hydrocarbon nodules in sandstones, and their significance for petroleum exploration. *J. Geol. Soc., Lond.*, **147**, 837–42.

Rimsaite, J. (1978) Layer silicates and clays in the Rabbit Lake uranium deposit, Saskatchewan. *Geol. Surv. Canada Current Research*, Part A, Paper **78-1A**, 303–15.

Rimsaite, J. (1982) Mode of occurrence of secondary radionuclide-bearing minerals in natural argillized rocks: A preliminary report related to a barrier clay in nuclear waste disposal. *Geol. Surv. Canada Current Research*, Part A, Paper **82-1A**, 247–59.

Rouzard, J.N., Oberlin, A. and Trichet, J. (1980) Interaction of uranium and organic matter in uraniferous sediments. In *Advances in Organic Geochemistry 1979*, A.G. Douglas, A.G. and J.R. Maxwell, eds. Pergamon Press, Oxford, 505–16.

Ruffenach, J.C., Hagemann, R. and Roth, E. (1980) Isotopic abundances measurements a key to understanding the Oklo phenomenon. *Zeits. Naturforsch.*, **35a**, 171–9.

Smits, G. (1992) Mineralogical evidence for geochemical environment at the earth's surface during deposition of Witwatersrand reefs. *Trans. Inst. Mining Metall. (Section B: Appl. Earth Sci.)*, **101**, 99–107.

[*Manuscript received 7 August 1995: revised 8 November 1995*]